

1 Collisional history of asteroid Itokawa

2 **F. Jourdan^{1*}, N.E. Timms², E. Eroglu¹, C. Mayers¹, A. Frew¹, P.A. Bland², G.S. Collins³,**
3 **T.M. Davison³, M. Abe⁴, and T. Yada⁴**

4 *¹Western Australian Argon Isotope Facility, Department of Applied Geology & JdL Centre,*
5 *Curtin University, Perth, WA 6845, Australia*

6 *²Department of Applied Geology, Curtin University, Perth WA 6845, Australia*

7 *³Impacts and Astromaterials Research Centre, Department of Earth Science and Engineering,*
8 *Imperial College, London SW7 2AZ, UK*

9 *⁴Institute of Space and Astronautical Science, Japan Aerospace Exploration Agency,*
10 *Sagamihara, Kanagawa 252-5210, Japan*

11 *E-mail: f.jourdan@curtin.edu.au

12 **ABSTRACT**

13 In situ extraterrestrial samples returned for study (e.g., from the Moon) are crucial in
14 understanding the origin and evolution of the Solar System as, contrary to meteorites, they
15 provide a known geological context for the samples and their analyses. Asteroid 25143 Itokawa
16 is a rubble pile asteroid consisting of reaccumulated fragments from a catastrophically disrupted
17 monolithic parent asteroid, and from which regolith dust particles have been recovered by the
18 Hayabusa space probe. We analyzed two dust particles using Electron Backscatter Diffraction
19 (EBSD) and $^{40}\text{Ar}/^{39}\text{Ar}$ dating techniques. One of the grains showing signs of 15–25 GPa impact
20 shock pressure, yielded a $^{40}\text{Ar}/^{39}\text{Ar}$ plateau age of 2.3 ± 0.1 Ga. We develop a novel temperature-
21 pressure-porosity model, coupled with diffusion models to show that the relatively low pressure
22 and high temperature involved in the impact process can be reconciled only if the asteroid was
23 already made of porous material at ~ 2.3 Ga and thus, if asteroid Itokawa was already formed,

24 thereby providing a minimum age for catastrophic asteroid breakup. A second particle shows no
25 sign of deformation indicating shock pressure of < 10 GPa and a calculated maximum
26 temperature of ~ 200 °C. This low temperature estimate is compatible with a lack of isotopic
27 resetting for this particle. This suggests that the breakup of Itokawa's parent was a relatively
28 low-temperature process at the scale of the asteroid, and occurred on a pre-shattered parent body.

29 INTRODUCTION

30 One of the main goals of the Hayabusa mission was to recover samples from asteroid
31 25143 Itokawa, a $535 \times 295 \times 209$ m body, and return them to the Earth (Abe et al., 2006;
32 Nakamura et al., 2011). In June 2010, the sample catcher was recovered revealing at least 1500
33 regolith particles, with the majority of them being significantly smaller than a hundred
34 micrometres (Nakamura et al., 2011; Tsuchiyama, 2014). The Itokawa particles are thus the first
35 and only extraterrestrial samples ever recovered from a known asteroid.

36 Petrographic inspection (Fig. 1; SI Materials and Methods), elemental and oxygen
37 isotope analyses revealed that particles from Itokawa are mostly made of olivine, low- and high-
38 Ca equilibrated pyroxene and albitic plagioclase, suggesting high temperature metamorphism of
39 grades 5 and 6, and that those particles are LL5 and LL6 equilibrated chondrites (Nakamura et
40 al., 2011; Nakashima et al., 2013). Equilibrium temperature calculations showed that these
41 minerals experienced a peak metamorphic temperature of ~ 800 °C during the formation of the
42 parent asteroid (Nakamura et al., 2011). Particles are either unshocked or show a variety of shock
43 signatures from lightly- to moderately-shocked (Nakamura et al., 2011) due to subsequent impact
44 events. Because the internal metamorphic temperatures are too high for a small Itokawa-size
45 body, and, because of its clear rubble pile structure (Tsuchiyama, 2014), it has been suggested
46 that the first-generation parent body of Itokawa must have been initially as large as a few tens of

47 kilometers, and has subsequently been destroyed by an impact (Nakamura et al., 2011). The
48 resulting fragments then reaccumulated to form a rubble pile asteroid (Michel and Richardson,
49 2013). An $^{40}\text{Ar}/^{39}\text{Ar}$ age of ~ 1.3 Ga was obtained by Park et al. (2015) which was unfortunately
50 derived from analyzing an uncharacterized mixture of three grains, each likely to have its own
51 time-temperature history, making any interpretation difficult.

52 When and how did the collision that resulted in the breakup of Itokawa's parent body
53 occur? In this study, we investigate the deformation (shock) state of the RA-QD02-0030 and
54 RA-QD02-0013 highly-equilibrated particles (Nakamura et al., 2011); hereafter #0030 and
55 #0013) which are two plagioclase + olivine + pyroxene composite grains of 165 μm and 91 μm
56 in diameter, respectively and with #0013 containing K-feldspar exolutions (full petrographic
57 descriptions are given in SI Materials and Methods). We used electron backscatter diffraction
58 (EBSD), alongside the first *single-grain* $^{40}\text{Ar}/^{39}\text{Ar}$ age dating analyses of extra-terrestrial dust
59 particles. These results give us some insight on the time-temperature (\pm shock) history of each of
60 those particles. To make sense of those data, we then developed a pressure-temperature-porosity
61 model that supports a low-energy impact process for the disruption of Itokawa's parent body,
62 and used an argon diffusion model to provide a minimum age for this event.

63 **RESULTS**

64 EBSD analyses show that the minerals from particle #0030 appear as irregularly shaped
65 and sized grains, with no crystallographic preferred orientations, common 120° triple junctions
66 and negligible intra-grain lattice strain, indicative of high-temperature textural equilibration (Fig.
67 1; SI Materials and Methods). Absence of glass, high-pressure polymorphs, mosaicism, planar
68 deformation features (PDFs) and extensive crack damage seems to indicate that this particle did
69 not experience significant shock. The presence of a few cracks (Fig. 1) might suggest a S1-S2

70 shock condition placing an upper limit of 5–10 GPa (Schmitt, 2000). In contrast, particle #0013
71 shows clear signs of deformation. Although no glass, high-pressure polymorphs, or PDFs were
72 observed, EBSD analyses showed that a large olivine crystal is strained and has up to 6°
73 variation in orientation (Fig. 1). The likely cause for such features in an asteroid particle is
74 shock. Signs of misorientation in olivine provide a minimum shock pressure estimate of 10–15
75 GPa when compared with artificial shock experiment observations (Schmitt, 2000). A maximum
76 pressure value of 25 GPa can be estimated, above which, experiments show that plagioclase
77 turns to diaplectic glass and above 30 GPa, pyroxene shows signs of mosaicism (Schmitt, 2000),
78 which are not observed.

79 Particle #0030 had the smallest argon yield of the two particles and this was clearly at the
80 limit of the technique and yielded plateau ages of 5.4 ± 1.6 Ga and 4.6 ± 1.8 Ga depending on the
81 blank correction applied (2σ ; Figure 2; SI Materials and Methods). These results suggest that the
82 formation age of the high temperature, equilibrated fabric of this particle is in fact very old.
83 Although the current data do not allow one to exactly calculate its formation age, the important
84 point is that the apparent old age is in agreement with the very low shock nature of particle
85 #0030, where no age resetting is expected. Particle #0013 yielded a well-defined plateau age of
86 2289 ± 139 Ma (2σ ; MSWD = 0.31, P = 1.0; Fig. 2). Two separate spikes of ^{39}Ar released (Fig.
87 2) are associated with the argon released first from the ca. 5 μm sized K-feldspar, and
88 subsequently from the 25 μm albite crystals, because albite has a higher activation energy than
89 K-feldspar (Cassata and Renne, 2013). A full plateau indicates that all of the radiogenic gas that
90 had accumulated before the impact involving the chondritic grain has been completely reset in
91 both phases during a thermal event at ~ 2.3 Ga. These data represent the first precise $^{40}\text{Ar}/^{39}\text{Ar}$
92 plateau age ever obtained from a single-grain dust particle recovered in situ from an asteroid.

93 **DISCUSSION**

94 Petrographic observations showed that most Itokawa dust particles experienced only very
95 low levels of shock (Nakamura et al., 2011), which a priori suggests low post-shock
96 temperatures. Shock heating in an asteroid collision is a strong function of initial porosity
97 (Davison et al., 2010). The energy expended compacting pore space is retained as waste heat,
98 which dramatically increases the post-shock temperature resulting from a given shock pressure
99 excursion, even for low to moderate shock events (Davison et al., 2016). To better understand
100 the significance of our data, we (1) used solid-state volume diffusion models to test the
101 maximum time-temperature conditions required to reproduce the $^{40}\text{Ar}/^{39}\text{Ar}$ age spectra for
102 particle #0030 (Fig. 3a) and (2), developed a novel shock-heating model based on the numerical
103 approach described by Davison et al. (2010) using forsterite as an analogue for the composition
104 of Itokawa to calculate the post-shock temperature as a function of peak-shock pressure and
105 porosity (Fig. 4). We ran our model for pressure values up to 70 GPa and initial porosity up to
106 40% and starting from a pre-shock temperature of 0 °C, (Fig. 4). We have calculated that pre-
107 shock ambient temperature of *buried* particles could vary between ca. 65 °C to –110 °C for a
108 variety of orbits (0.5–1.7 AU), but this would affect our porosity estimate by less than 5% (Fig.
109 4).

110 Our model suggests that the low level of pressure experienced by particle #0030 (max. \leq
111 10 GPa) corresponds to a maximum temperature of ca. 200 °C for a target rock with a porosity of
112 10% (Fig. 3), the latter value being similar to most chondrites and expected for a post-
113 compaction (pre-breakup) 4.5 Ga old chondritic asteroid (Consolmagno et al., 2008). Our
114 diffusion models suggest that such a low (and brief) spike in temperature would not be sufficient
115 to reset the K/Ar isotopic clock in feldspar which can withstand temperature spikes up to 500°C

116 before being noticeably affected (Fig. 3a). This is in agreement with (but does not rely upon) the
117 apparent lack of isotopic resetting shown by the $^{40}\text{Ar}/^{39}\text{Ar}$ age of particle #0030 (Fig. 2). This
118 suggests that the final disruption (breakup) of the proto-Itokawa asteroid was globally a
119 relatively low-temperature process, with some areas not heated above 200 °C. This is in excellent
120 agreement with breakup models of structurally weakened monolith asteroids (Michel et al.,
121 2004a, b) where asteroids have been suggested to be pre-shattered by continuous battering by
122 small impacts and more prone to breakup, even by a final low-energy impact.

123 EBSD and $^{40}\text{Ar}/^{39}\text{Ar}$ analyses of particle #0013 suggest a localized impact event with
124 sufficient energy to fully reset the K/Ar system in plagioclase and K-feldspar at ~2.3 Ga. To
125 estimate the heating conditions (minimum temperature coupled with cooling duration) that can
126 reproduce the reset $^{40}\text{Ar}/^{39}\text{Ar}$ age spectrum of particle #0013, we calculated the post-impact
127 cooling duration of a chondrite boulder of 25 m radius (similar to size of the biggest boulders at
128 the surface of Itokawa; Tsuchiyama, 2014) from peak post-shock temperatures of 900 °C to
129 below 200 °C following the approach of Humayun and Koeberl (2004), and considering that
130 particle #0013 is buried in the boulder at an unknown depth. We iteratively coupled these results
131 with our solid-state diffusion model discussed above (Fig. 3; SI Materials and Methods for
132 details). Our models show that a post-shock temperature greater than ~900 °C associated with a
133 cooling duration of 12.5 days are necessary to fully reset the K/Ar system. For the low ($\leq 10\%$)
134 porosity material expected to be found in Itokawa's monolithic parent body prior to breakup
135 (Consolmagno et al., 2008; Michel and Richardson, 2013), a post-shock temperature of 900 °C
136 would imply shock levels >50 GPa (Fig. 4), which is inconsistent with petrographic
137 observations. However, our pressure-temperature-porosity model suggests that impact shock
138 pressure of 15–25 GPa can produce post-shock temperatures of 900 °C, provided that the target

139 material had an initial porosity of at least 20%–30% (Fig. 4). Such a high porosity level is more
140 likely compatible with the average porosity of a rubble pile asteroid (~40% for Itokawa;
141 Tsuchiyama, 2014).

142 Therefore, those results imply that the high-porosity rubble pile structure seen today
143 already existed at ~2.3 Ga, which provides a *minimum* age for the breakup event of the
144 monolithic proto-Itokawa parent body and the formation of the rubble-pile Itokawa. The two
145 particles then resided at least few meters in the regolith layer until they surfaced less than 10
146 million years ago as indicated by cosmogenic nuclides obtained on several other particles (Nagao
147 et al., 2011).

148 CONCLUSIONS

149 In this study, petrographic and EBSD observations, $^{40}\text{Ar}/^{39}\text{Ar}$ analyses, pressure-
150 temperature-porosity models and solid-state argon diffusion models provide coherent constraints
151 and suggest that the breakup of Itokawa's monolithic parent body (formed at 4.5 Ga) occurred
152 more than 2.3 billion years ago and was a relatively low temperature process caused by a
153 moderate sized impact occurring on a pre-shattered parent body.

154 ACKNOWLEDGMENTS

155 We thank an anonymous reviewer, D. Nakashima and K. Min for their
156 constructive reviews, and editor D. Brown.

157

158

159 REFERENCES CITED

- 160 Abe, M., et al., 2006, Near-infrared spectral results of asteroid Itokawa from the Hayabusa
161 spacecraft: *Science*, v. 312, p. 1334–1338.
- 162 Benz, W., Cameron, A.G.W., and Melosh, H.J., 1989, The origin of the Moon and the single-
163 impact hypothesis III: *Icarus*, v. 81, p. 113–131, doi:10.1016/0019-1035(89)90129-2.

- 164 Cassata, W.S., and Renne, P.R., 2013, Systematic variations of argon diffusion in feldspars and
165 implications for thermochronometry: *Geochimica et Cosmochimica Acta*, v. 112, p. 251–
166 287, doi:10.1016/j.gca.2013.02.030.
- 167 Consolmagno, G., Britt, D., and Macke, R., 2008, The significance of meteorite density and
168 porosity: *Chemie der Erde-Geochemistry*, v. 68, p. 1–29, doi:10.1016/j.chemer.2008.01.003.
- 169 Crank, J., and Gupta, R.S., 1975, Isotherm Migration Method in 2 Dimensions: *International*
170 *Journal of Heat and Mass Transfer*, v. 18, p. 1101–1107, doi:10.1016/0017-9310(75)90228-
171 8.
- 172 Davison, T.M., Collins, G.S., and Ciesla, F.J., 2010, Numerical modelling of heating in porous
173 planetesimal collisions: *Icarus*, v. 208, p. 468–481, doi:10.1016/j.icarus.2010.01.034.
- 174 Davison T. M., Collins G. S., and Bland P. A. 2016. Mesoscale Modeling of Impact Compaction
175 of Primitive Solar System Solids. *The Astrophysical Journal* 821:68.
- 176 Humayun, M., and Koeberl, C., 2004, Potassium isotopic composition of Australasian tektites:
177 *Meteoritics & Planetary Science*, v. 39, p. 1509–1516, doi:10.1111/j.1945-
178 5100.2004.tb00125.x.
- 179 McDougall, I., and Harrison, T.M., 1999, *Geochronology and thermochronology by the*
180 *⁴⁰Ar/³⁹Ar method*: Oxford, New York, Oxford University Press, 269 p.
- 181 Michel, P., Benz, W., and Richardson, D.C., 2004a, Catastrophic disruption of asteroids and
182 family formation: A review of numerical simulations including both fragmentation and
183 gravitational reaccumulations: *Planetary and Space Science*, v. 52, p. 1109–1117,
184 doi:10.1016/j.pss.2004.07.008.
- 185 -, 2004b, Catastrophic disruption of pre-shattered parent bodies: *Icarus*, v. 168, p. 420–432,
186 doi:10.1016/j.icarus.2003.12.011.

- 187 Michel, P., and Richardson, D.C., 2013, Collision and gravitational reaccumulation: Possible
188 formation mechanism of the asteroid Itokawa: *Astronomy and Astrophysics*, v. 554, p. L1–
189 L4, doi:10.1051/0004-6361/201321657.
- 190 Nagao, K., Okazaki, R., Nakamura, T., Miura, Y.N., Osawa, T., Bajo, K.-i., Matsuda, S.,
191 Ebihara, M., Ireland, T.R., and Kitajima, F., 2011, Irradiation history of Itokawa regolith
192 material deduced from noble gases in the Hayabusa samples: *Science*, v. 333, p. 1128–1131,
193 doi:10.1126/science.1207785.
- 194 Nakamura, T., et al., 2011, Itokawa dust particles: A direct link between S-type asteroids and
195 ordinary chondrites: *Science*, v. 333, p. 1113–1116, doi:10.1126/science.1207758.
- 196 Nakashima, D., Kita, N.T., Ushikubo, T., Noguchi, T., Nakamura, T., and Valley, J.W., 2013,
197 Oxygen three-isotope ratios of silicate particles returned from asteroid Itokawa by the
198 Hayabusa spacecraft: A strong link with equilibrated LL chondrites: *Earth and Planetary
199 Science Letters*, v. 379, p. 127–136, doi:10.1016/j.epsl.2013.08.009.
- 200 Park, J., Turrin, B.D., Herzog, G.F., Lindsay, F.N., Delaney, J.S., Swisher, C.C., Uesugi, M.,
201 Karouji, Y., Yada, T., and Abe, M., 2015, $^{40}\text{Ar}/^{39}\text{Ar}$ age of material returned from asteroid
202 25143 Itokawa: *Meteoritics & Planetary Science*, v. 50, p. 2087–2098,
203 doi:10.1111/maps.12564.
- 204 Schmitt, R.T., 2000, Shock experiments with the H6 chondrite Kernouve: Pressure calibration of
205 microscopic shock effects: *Meteoritics & Planetary Science*, v. 35, p. 545–560,
206 doi:10.1111/j.1945-5100.2000.tb01435.x.
- 207 Tsuchiyama, A., 2014, Asteroid Itokawa a source of ordinary chondrites and a laboratory for
208 surface processes: *Elements*, v. 10, p. 45–50, doi:10.2113/gselements.10.1.45.

209 FIGURE CAPTIONS

210 Figure 1. Crystallographic orientation maps measured by Electron Back Scatter Diffraction
211 (EBSD). A) particle #0030; B) particle #0013; C) enlarged portion panel B). The particles
212 contain olivine (Ol), low- and high-Ca pyroxene (L-Px, H-Px), plagioclase (Pl), K-feldspar (K-
213 Fd), chromite (Chr), taenite (Tae) and kamacite (Kam). Phases in (A) and (B) are colored using
214 an Euler color scheme. Olivine in (B) and (C) is colored for crystallographic misorientation from
215 a reference point (red cross), and shows up to 6° of lattice strain. Greyscale of feldspar in C
216 reflects crystallinity (pale = stronger EBSD patterns), and reveals planar fractures (white
217 triangles). Detailed procedure and results are provided in the Supplementary Information.

218 Figure 2. Single-grain laser step-heating $^{40}\text{Ar}/^{39}\text{Ar}$ age spectra of particles #0030 and #0013
219 measured on the ARGUS VI mass spectrometer. Note that #0030 yielded plateau ages of $\sim 5.4 \pm$
220 1.6 Ga for blank correction #2 or and 4.6 ± 1.8 Ga for blank correction #1 (not shown). The solid
221 line indicates the width of the plateau age (i.e., the steps included in the calculation). Detailed
222 procedure and results are provided in the SI Materials and Methods.

223 Figure 3. Modeled age spectra based on the diffusion equations of Crank and Gupta (1975) and
224 McDougall and Harrison (1999) for a mixture comprising a $25 \mu\text{m}$ radius sphere with an albite
225 composition and a $5 \mu\text{m}$ radius sphere with a K-feldspar composition that has been heated at peak
226 temperatures ranging from 500°C to 900°C . Cooling from the peak temperature to 200°C is
227 simulated over 12.5 days (cf. Supplementary information). Blue areas represent age spectrum
228 envelopes from Fig. 2.

229 Figure 4. Post-shock temperature of forsterite as a function of shock pressure for a range of
230 different initial porosities (ϕ). Shock and release calculations computed using ANEOS
231 (ANalytical Equation Of State) for forsterite (Benz et al., 1989), following the approach
232 described by (Davison et al., 2010). Temperatures above the solidus (dashed lines) are

233 approximate as latent heat of fusion is neglected. Horizontal lines indicate the upper and lower
234 bounds on heating inferred from K/Ar system resetting.
235 1GSA Data Repository item 2017xxx, xxxxxxxx, is available online at
236 <http://www.geosociety.org/datarepository/2017/> or on request from editing@geosociety.org.

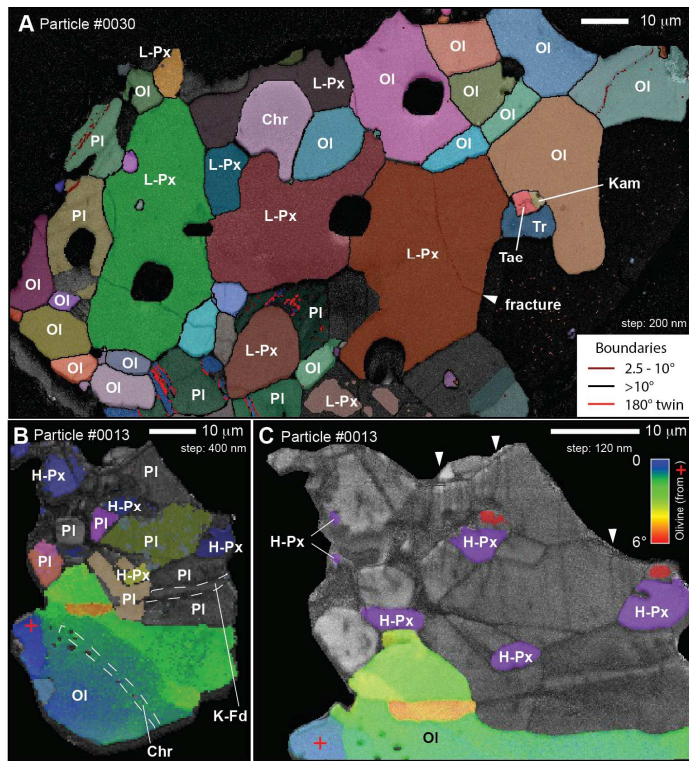


Fig. 1: Jourdan et al.

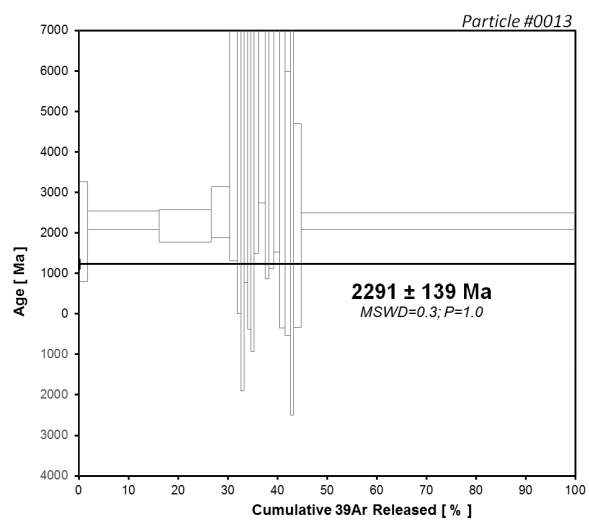
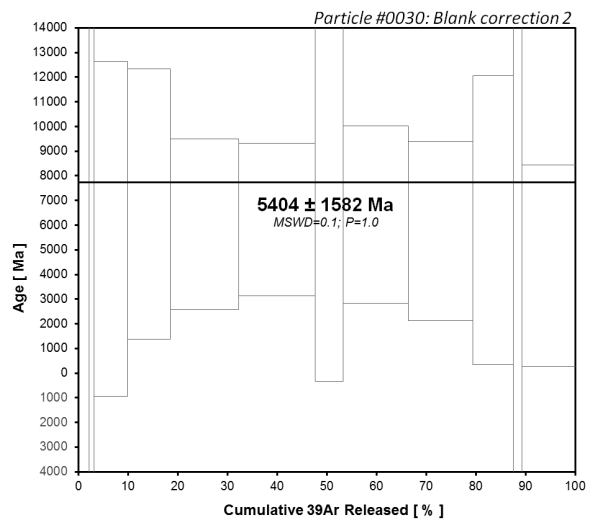


Fig. 2: Jourdan et al.

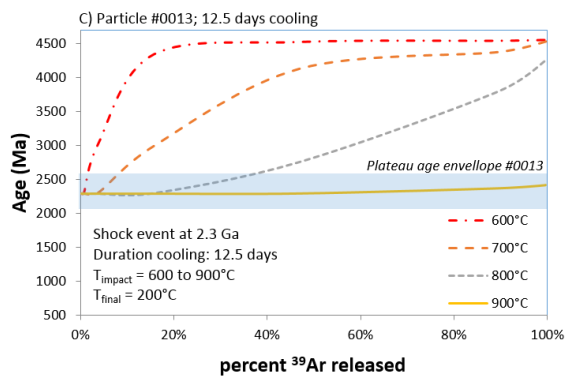
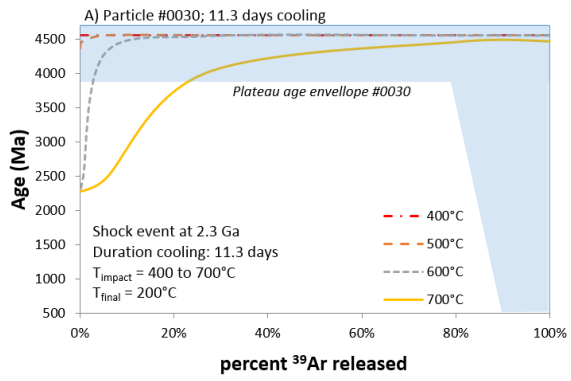


Fig. 3: Jourdan et al.

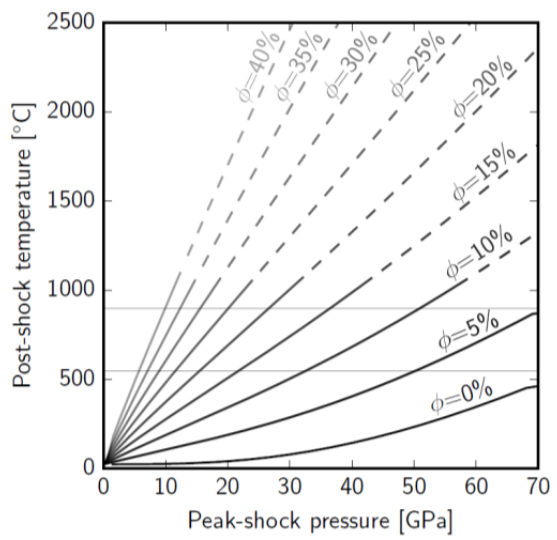


Fig . 4: Jourdan et al.